Colloid Polym Sci (2005) 283: 402–412
DOI 10.1007/s00396-004-1161-9

ORIGINAL CONTRIBUTION

Gemma Montalvo
Ali Khan

Rheological properties of a surfactant-induced gel for the lysozyme–sodium dodecyl sulfate–water system

Received: 16 December 2003
Accepted: 18 May 2004
Published online: 7 July 2004

G. Montalvo (✉)
Departamento de Química Física,
Universidad de Alcalá, 28871
Alcalá de Henares, Madrid, Spain
E-mail: gemma.montalvo@uah.es

A. Khan
Physical Chemistry 1, Center for Chemistry and Chemical Engineering,
Lund University, P.O. Box 124,
22100 Lund, Sweden

Abstract Rheological properties of isotropic solutions and gel structures of lysozyme–sodium dodecyl sulfate mixtures in water are investigated. Isotropic solutions behave as Newtonian fluids with very low viscosity values. For the lysozyme solutions the intrinsic viscosity and the Huggins coefficient were calculated on the basis of the Mooney equation. Above a certain yield stress value, the viscosity of the gel samples decreases continuously in the whole range of the shear rate. Dynamic rheological experiments show weak gel behavior where the storage modulus and the loss modulus are almost parallel and are frequency-dependent. A belated gel stage with very slow kinetics has been characterized. There is a substantial enhancement of the gel strength by ageing since the belated gel stage manifests a higher yield stress value and a higher storage modulus than the initial gel stage. The gels are stable in the temperature range between 10 and 32 °C.

Keywords Protein–surfactant interactions · Lysozyme · Sodium dodecyl sulfate · Isotropic solution · Weak gel · Rheology

Introduction

Protein gels can be prepared by different treatments, such as acidification, enzymatic reaction, and simply by heating the aqueous solution of proteins [1, 2, 3, 4, 5]. Of these, heat-set gels of single and mixed globular proteins have been extensively studied [1, 2, 3, 4, 5, 6, 7, 8, 9, 10, 11, 12]. Once the gel is formed by thermal treatment, the process is not reversible. Mainly two kinds of heat-set gels are observed: one a transparent gel and the other a nontransparent gel [5]. The transparent gel consists of a molecular homogeneous network. The network is built up by extended strings or beads as a result of a long-range order, which is induced by the charge of the protein. When the charge of the protein is decreased, the electrostatic long-range forces are reduced. It is suggested to produce the nontransparent gel consisting of a randomly aggregation protein network [3, 11, 13]. Moreover, although the heat-set gels can be formed with great differences in microstructures as very stranded or very particulate, these materials may have similar macroscopical properties such as rheological behavior, i.e., mechanical and viscoelastic properties [14, 15]. A gel is rheologically characterized by the storage modulus, G', nearly independent of the angular frequency and the values of the loss modulus, G'', are at least 1 decade lower than the G' values. However, gel materials may also be characterized rheologically as ''weak gels''. The mechanical spectra of a weak gel are slightly different from those of conventional gels in several respects: there is a small linear viscoelastic region; the G' and G'' moduli are frequency-dependent and at the maximum, the G' values are higher by 1 order of magnitude compared with the G'' values [16, 17, 18, 19].

Recently, materials with the macroscopical appearance of a gel have been discovered by mixing globular

proteins and oppositely charged surfactants at room temperature. A few examples of the systems that produce this type of gel are lysozyme–sodium dodecyl sulfate (SDS)–water [20], β-lactoglobulin–dodecyltrimethylammonium chloride (DOTAC)–water [21], ovalbumin–DOTAC–water [22], lysozyme–lithium perfluorononanoate–water [23], and bovine serum albumin–sodium taurodeoxycholate–water [23]. Among these systems, the gel phase formed by the lysozyme–SDS–water system has been studied in detail in terms of its formation, stability, and structure [20, 22, 24, 25, 26, 27, 28]; however, the macroscopic properties of the system have not been studied in any detail. Here, we attempted to clarify whether the novel gel phase behaves mechanically as a gel and to evaluate the possibility of the gel material for future technical applications.

Addition of SDS to an aqueous solution of lysozyme causes precipitation that, on adding more SDS, transforms it into a gel. This gel redissolves on further addition of SDS and the protein–surfactant complexes are assembled into micellar aggregates. The gel coexists with the precipitate and solution phase by the appropriate two- and three-phase regions. The homogeneous single gel phase is considered thermodynamically stable. Macroscopically, the gel material is isotropic, slightly turbid, and can be prepared by following different routes. Concerning the structure, the solution phase consists of small aggregates, while large domains of an approximately 500-nm size were detected in the gel phase by ^{2}H NMR relaxation [22] and cryogenic transmission electron microscopy (cryo-TEM) [26] techniques. Moreover, small-angle neutron scattering (SANS) indicates that the gel is built up by structural cluster subunits of eight densely packed lysozyme–surfactant complexes [28]. There is a one-dimensional growth in a global structure that is not very fractal. Furthermore, the protein retrains its globular size and there are no free surfactant micelles in the gel structure [22]. Hence, the heat-set globular proteins are structurally different in this aspect, since an unfolding protein process is required before their aggregation [2].

On the other hand, the gelling process is one of the most important mechanisms for developing structures with desirable mechanical properties that are suitable for practical applications. In the literature there are very few studies that consider sol–gel transitions in highly concentrated protein–surfactant systems at room temperature [29]. In particular, systems of oppositely charged protein–surfactant gels still are incomprehensive. The gelling behavior of the lysozyme–SDS–water is system very different compared with the heat-set gels of single and mixed protein systems [14, 30, 31, 32]. Instead of a fast gelling process of a few hours, the addition of the surfactant to the lysozyme solution induces a bluish solution that precedes the formation of the gel. The sol–gel transition in lysozyme–SDS mixtures occurs within about 1 week.

In this work, we studied the mechanical properties of the isotropic solution and gel phases of the lysozyme–SDS–water system by rheology. The peculiarities of this surfactant-induced gel compared with the heat-set gels, such as (1) thermodynamically stable equilibrium with other phases, (2) a reversible gel process, and (3) the globular size of the protein, motivated us to study this system. The effects of ageing, composition, and temperature on the gel are examined. Direct observation of the microstructure may be necessary in order to understand the mechanical behavior. So, although the relationship between structure and rheology remains poorly understood we correlated these observations, taking into account the previous results obtained by a combination of different experimental techniques, such as optical polarizing microscopy, NMR, Raman spectroscopy, SANS, and cryo-TEM [20, 22, 24, 26, 27, 28]. In this study, we are interested in the gel material instead of the lysozyme activity. Once the gelling process is well characterized, the practical applications of this gel-like material in pharmaceutical, cosmetic or food formulations can be developed in future studies.

Experimental

Materials

Lysozyme from chicken egg white no. L-6876, crystallized three times, dialyzed, and lyophilized was used as supplied from Sigma. It is very stable within a large pH range and contains about 5 wt % of sodium acetate and sodium chloride salt buffers. SDS (especially pure) was purchased from BDH Chemicals (Poole, UK) and Millipore-filtered-quality water was used as a solvent. The difference in pH was negligibly small among all the protein samples and it was considered to be constant at pH 6.5.

Sample preparation

Samples were prepared by weighing the desired amounts of stock solutions of protein and surfactant into screw-capped vials. After an initial vigorous vortexing, the samples were put in a shaker for a few days. The gel samples were left to equilibrate at 25.0 °C for at least 1 month prior to starting the rheological experiments, while isotropic solutions attained equilibrium within a few days.

Methods

Ubbelohde capillary viscometer

The viscosity of the isotropic solutions of the pure lysozyme–water system was measured using a Ubbelohde capillary viscometer connected to an automatic time counter, Schott-Geräte AVS400, and to a water bath, Schott Geräte CT1150, which controlled the temperature. The viscosity is obtained by Eq. (1):

$$\eta = c\rho t, \tag{1}$$

where c is the viscometer constant with a value of 0.03075 $mm^2\ s^{-2}$ and t is the time taken for the gravity-driven flow to move from one vertical position to another. The densities of the samples, ρ, were calculated using a pycnometer.

Rheometry

Rheological measurements were performed for the isotropic solution and the gel samples with a Carri-Med CSL 100 controlled-stress rheometer using cone–plate geometry. The acrylic cone had an angle of 1° and its diameter was 4 cm. The measurements of the gel samples were also performed in a parallel steel plate geometry with a gap larger than 1,200 μm and a plate diameter of 2 cm. The data from different additions and different geometry configurations were obtained with good accuracy and reproducibility. The temperature of the system was maintained at 25.0 °C by a Peltier system and a humidification chamber containing wetted sponges was used to prevent the evaporation of the sample during the measurement. The sample compression during loading was done at the lowest rate to minimize its perturbation.

In the flow experiments, viscosity values were obtained as the rate of change of shear stress with respect to shear rate. For the isotropic solution, the viscosity values were studied as a function of volume fraction, ϕ, which was calculated by

$$\phi = \frac{(v_{\mathrm{DS}}\text{ - }w_{\mathrm{SDS}})/M_{\mathrm{DS}}\text{ - } + (v_{\mathrm{Lys}}w_{\mathrm{Lys}})/M_{\mathrm{Lys}}}{(v_{\mathrm{SDS}}w_{\mathrm{SDS}})/M_{\mathrm{SDS}} + (v_{\mathrm{Lys}}w_{\mathrm{Lys}})/M_{\mathrm{Lys}} + (v_{\mathrm{w}}w_{\mathrm{w}})/M_{\mathrm{w}}}, \tag{2}$$

where w is the weight fraction, and M is the molecular weight of the different components assigned as lysozyme (Lys), surfactant (SDS), hydrocarbon chain of the surfactant (DS^-) and water (w); v is the molecular volume and we used the values $v_{\mathrm{Lys}} = 16{,}963.6\ Å^3$, [33] $v_{\mathrm{DS}^-} = 400.3\ Å^3$ [34], $v_{\mathrm{SDS}} = 414.5\ Å^3$ [34] and $v_{\mathrm{w}} = 30.0\ Å^3$.

Structural parameters such as the dynamic storage modulus (G') and the loss modulus (G'') were recorded as a function of the angular frequency ω ($\omega = 2\pi f$) in the range $f = 0.005$–40 Hz and at a constant stress. G' and G'' are the two components of the complex modulus G^* (ratio of stress amplitude to strain amplitude). They are connected to the complex viscosity through Eq. (3):

$$\eta^* = \frac{\sqrt{G'^2 + G''^2}}{\omega}, \tag{3}$$

All measurements were carried out in the regime of linear viscoelasticity, i.e., where the material parameters are independent of the applied stress.

The temperature effect on the gel structure was studied in the range from 10 to 40 °C, at a frequency of 0.1 Hz, except for the sample that contains 11.9 wt % of lysozyme, for which a frequency of 1 Hz was used. A period of 10 min was allowed for the thermal equilibration, before starting the experiment, for all samples.

Results and discussion

The lysozyme–SDS—water system was studied below 20 wt % of both protein and surfactant. The phase diagram (Fig. 1) is dominated by a clear and isotropic solution phase at high SDS concentration; at low SDS concentration there is a white precipitate in equilibrium with the solution phase. A single gel phase is formed in a narrow strip between the precipitation region and the solution phase. The single phases coexist through the appropriate two- and three-phase regions [20].

The aim of the rheological experiments is to characterize the viscoelastic behavior of the aggregates formed by the protein–surfactant mixtures in the solution phase as well as in the gel phase. We carried out a systematic study on the aqueous solution of SDS and lysozyme, followed by one on the mixed protein–surfactant solution under different experimental conditions. Finally, we made a detailed study on the gel phase. The experiments were carried out at different water contents for the samples given in Fig. 1 with a constant molar ratio between surfactant and protein. For the solution phase, it was possible to choose a large variation of the surfactant-to-protein ratio, whereas for the gel phase, variation of the surfactant-to-protein ratio was limited since the width of the gel phase in terms of SDS concentration is very narrow.

Isotropic solutions: flow experiments

Binary systems

Samples of the isotropic solutions of both binary systems, SDS–water and lysozyme–water (measured by rheology as well) have viscosity values independent of

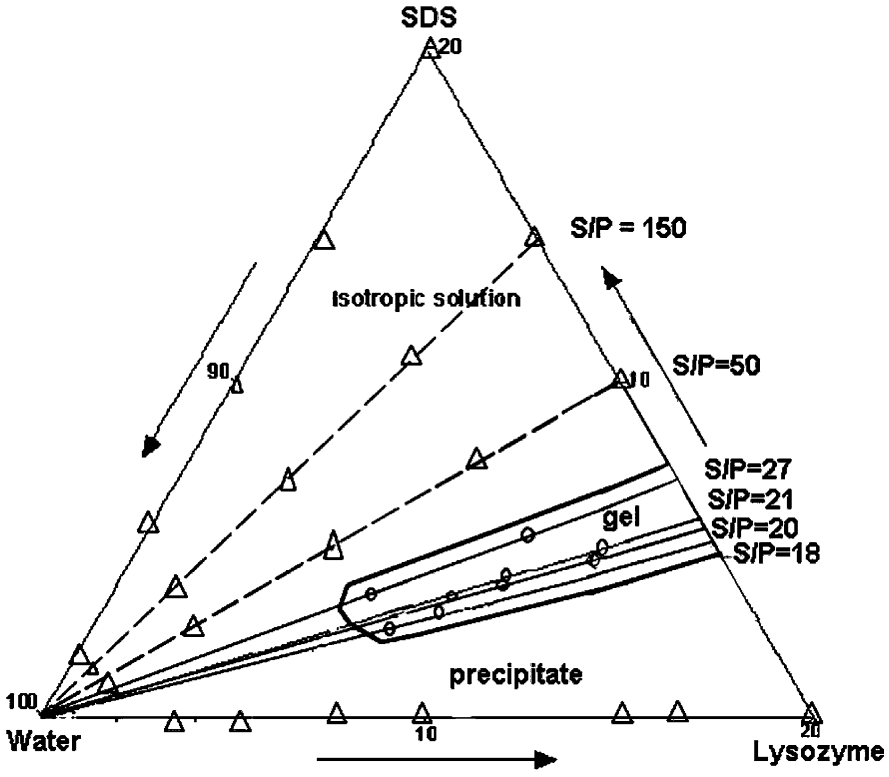

Fig. 1 Measured samples for the lysozyme–sodium dodecyl sulfate (*SDS*)–water system at constant surfactant-to-protein (*S*/*P*) molar ratio at 25 °C: isotropic solution (*triangles*); gel phase (*circles*). For the complete phase diagram, see Ref. [20]

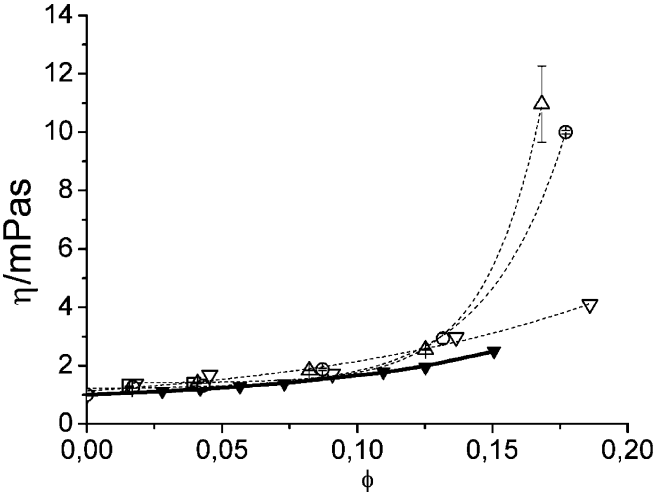

Fig. 2 Viscosity (η) as a function of surfactant or protein volume fraction (ϕ) for the binary systems, and total (surfactant plus protein) volume fraction for the ternary system, at 25 °C. Pure SDS (*open down triangles*); pure lysozyme (*closed down triangles*); S/P = 150 (*circles*); S/P = 50 (*up triangles*); S/P = 27 (*squares*). The *dashed lines* are guides for the eye. For the pure lysozyme aqueous system the *straight line* corresponds to the fit to Eq. (4)

the shear rate, indicating the Newtonian behavior of the solution phase. The micellar aggregates are not elongated as shearing does not orient them. The viscosity values (η) with their error bars are plotted against the sample composition as the volume fraction (ϕ) in Fig. 2. Both the systems recorded low values and η lies within the same order of water viscosity (1.0 mPa s).

For the pure SDS–water system, $\eta \sim 1.4$ mPa s obtained at 2 wt % of surfactant increased to $\eta \sim 4.1$ mPa s at 20 wt % of SDS (Fig. 2). The micellar phase of SDS has been studied extensively by a variety of experimental techniques [35, 36]. It has been concluded that in the absence of salt the micelles are small without undergoing any substantial micellar growth. The small η values in Fig. 2 are in accord with small micellar aggregates. A slight increase of the measured viscosity value with increased surfactant concentration may be due to the increase in the number of micelles in combination with a slight increase of the micellar size.

If the pure SDS micelles behave as single spherical and noninteracting particles in the dilute regime, the viscosity should be given by the classical Einstein equation, $\eta = \eta_s(1 + 2.5\phi)$, where η_s is the viscosity of water [37]. However, neither data fit that expression or the corrected equation given by Batchelor that considers a two-body hydrodynamic interaction between hard spheres, $\eta = \eta_s(1 + 2.5\phi + 6.2\phi^2)$. Hence, higher-order terms than ϕ^2 are expected owing to strong repulsive intermicellar interactions in the pure SDS–water system. While at low concentrations the nonlinear terms are negligible, at higher concentrations they become significant.

The viscosity of lysozyme solution is lower than that of the surfactant over the whole concentration range (Fig. 2). A slow increase of viscosity with increasing amount of protein was measured until about 7–10 wt % of lysozyme (i.e., $\phi < 0.07$ in Fig. 2). Over that protein content, the increase in the viscosity is more pronounced. The results may be understood in terms of monomer protein molecules at low protein concentration followed by oligomerization of protein with the increased concentration. This observation agrees well with previous results [38] as well as with our observations on the system by the SANS technique [28]. The SANS spectrum of lysozyme–water solution can be described by a combination of a hard sphere and a screened Coulomb potential for concentrations up to at least 10 wt %. At higher volume fractions, there is an increase in scattered intensity in the lower q range, which indicates the presence of oligomer aggregates.

In the particular case of aqueous solutions of globular proteins, it has been shown for a given temperature that the dependence of the relative viscosity (η_r) on concentration can be analyzed over the whole range of composition by the Mooney equation [39] as

$$\eta_r = \exp\left(\frac{S\phi}{1 - K\phi}\right), \tag{4}$$

where $\eta_r = \eta/\eta_s$ (η_s is the viscosity of water and η is that of the solution); ϕ is the volume fraction of the dissolved particles; K is a self-crowding factor; and S denotes the shape parameter of proteins in solution.

Note that for dilute solutions (i.e., $\phi \to 0$) and hard spherical particles ($S = 2.5$), Eq. (4) is the same as the well-known relation given by Einstein [37]. However, it has been proven that lysozyme molecules in aqueous solution behave as hard, quasi-spherical particles [40]. The viscosity values obtained experimentally for the lysozyme–water system fit well to the Mooney model, as shown in Fig. 2, with $K = 2.91$ and $S = 3.44$. At low concentration, an expansion of Eq. (4) in a power series of the concentration yields the following polynomial:

$$\frac{\eta_{sp}}{c} = [\eta]\left(1 + k_1[\eta]c + k_2[\eta]^2c^2 + k_3[\eta]^3c^3 + ...\right), \tag{5}$$

where $[\eta]$ is the intrinsic viscosity $\left([\eta] = \lim_{c\to 0}\frac{\eta_{sp}}{c}\right)$, with a value of 2.86×10^{-3} m^3 kg^{-1} for the lysozyme data fitting; η_{sp} is the specific viscosity ($\eta_{sp} = \eta_r - 1$); k_1 is the Huggins coefficient with a value of 1.18; and k_2, k_3, etc. are the higher coefficients of expansion, connected with the Huggins coefficient k_1 [40]. Both the S value and the intrinsic viscosity are slightly higher than the values reported previously in the literature [40, 41].

For globular proteins a dependence of the specific viscosity on the reduced concentration $c[\eta]$ has also been shown in a log–log plot that exhibits a clear transition from the dilute to semidilute region at some critical concentration c^* [42] or two critical concentrations from the dilute region to the concentrated region, c^* and c^{**} [41]. In the dilute and concentrated regions the dependence is linear with different slopes. For the lysozyme–water system, the plot given in Fig. 3a indicates a dilute region with a slope of 1.1, similar to those obtained for ovalbumin [42] and other kinds of molecules such as polysaccharides [43], cellulose derivatives [44] or native mammalian hemoglobins [45]. The semidilute domain extends over the critical concentration of $c^* = 60$ kg m^3 ($\phi \approx 0.05$, i.e., 7–8 wt % of lysozyme) and the relative viscosity can be described here by the Lefebvre equation [41],

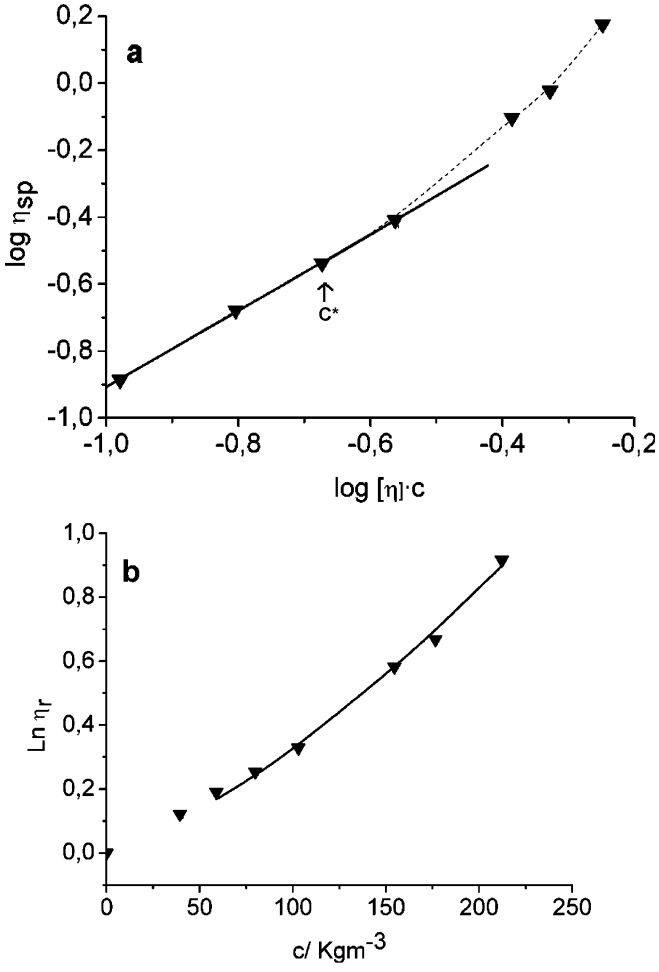

Fig. 3 **a** Specific viscosity as a function of the reduced concentration $c[\eta]$ in a log–log plot for the lysozyme–water system. The *dashed lines* are guides for the eye, and the *straight line* corresponds to the fit to Eq. (5) for the dilute regime. c^* and the *arrow* show the boundary concentration range from the dilute to the semidilute region. **b** Relative viscosity as a function of concentration in a log plot in the semidilute region for the lysozyme–water system. The *curve* shows the fit obtained by using Eq. (6)

$$\ln \eta_r = 2a[\eta]c^* \left(\frac{c}{c^*}\right)^{1/2a} - (2a-1)[\eta]c^*, \quad (6)$$

where a is the Mark–Houvink–Kuhn–Sakurada exponent. The experimental data in the semidilute domain fit well to this expression (Fig. 3b), taking c^* from the master curve (Fig. 3a), and the exponent a is the only adjustable parameter in Eq. (6). A value of $a = 0.32$ is in agreement with hard, quasi-spherical particles in solution, similar to ovalbumin [42] or mammalian hemoglobins [45].

Ternary system

Isotropic solutions in the lysozyme–SDS–water ternary system also exhibit Newtonian behavior with low viscosity values. At a constant amount of water, the viscosity values of the samples measured in the ternary system are clearly higher than those of the binary lysozyme–water system (Fig. 2). Our rheological results indicate that the addition of SDS to lysozyme solution induces aggregation, owing to strong electrostatic attraction between the positively charged protein and the negatively charged SDS molecules. It is interesting to note that the viscosity values are nearly independent of the surfactant-to-protein ratio (Fig. 2). Almost identical η values were measured for the surfactant–protein complex as well as for the pure SDS micellar solution; however, at $\phi > 0.13$, the increase of viscosity for the ternary solution is much larger than that of SDS micellar solution. It has been observed by a number of experimental techniques such as cryo-TEM [26], ^{2}H NMR [22], light scattering [46, 47, 48] and SANS [28, 49] that the ternary solution at $\phi > 0.10$ consists of a soluble surfactant–protein complex in equilibrium with free pure surfactant micelles. It seems that this system presents different kinds of interactions: attractive interactions between protein–protein molecules and protein–surfactant complexes; repulsive interactions between SDS micelles. The repulsive interactions are responsible for the samples not separating and remaining visually unchanged over the years.

Gel phase: flow experiments

The single gel phase has long-term stability. The samples in the gel phase were prepared and treated for running the flow experiments at a series of compositions with surfactant-to-protein ratios of 20 and 21 (Fig. 1) by following the procedure described earlier (Experimental section).

Upon applying a stress to the gel samples, initially they behave like a solid, i.e., they do not flow. The minimum stress which is required to initiate the flow of the sample is taken as the yield-stress value (σ_0), which was estimated from the flow curve by simple extrapolation to zero shear rate (Table 1). This solid behavior can be due to different kinds of interactions between the molecules, which may originate from a network throughout the sample volume [50]. The network is still able either to flow or to break down when stresses are applied. However, since the microfractures in the broken gel will lead to lumpy aggregates in the shear geometry, a laminar flow cannot be taken for granted anymore. This unstable flow situation is observed in the flow curves (Fig. 4). This phenomenon may be responsible for the data points that are not equally distributed and also for the rather bumpy flow curves. The viscosity, η, decreases continuously in the whole range of the shear rate, $\dot{\gamma}$. A similar trend has been observed with protein solutions [51] containing anionic surfactants [52] and it was attributed to the slow breaking down of the protein–surfactant complex by shearing [53].

Although the experiments correspond to a narrow SDS composition area, the viscosity values at a fixed shear rate clearly increase on decreasing the water content in the sample (Table 1). The yield stress values (σ_0) range from 15 to 210 Pa. At nearly constant amount of water the σ_0 values have the same order of magnitude in both series (Table 1). However, a slight tendency to higher yield stress and lower viscosity in the whole range of shear rate can be noted for samples with the lowest surfactant-to-protein ratio. The higher yield stress values for the series with a surfactant-to-protein ratio of 20 may relate to a more structured network of the gel.

Oscillation experiments

The oscillation experiments for the gel samples were carried out in the linear viscoelastic regime for the series at constant SDS–lysozyme molar ratio, ranging from 18 to 27 (Fig. 1). They were done between 1 and 3 months after the sample preparations. The profiles of the storage

Table 1 Yield stress values (σ_o) and viscosity (η), at $\dot{\gamma} = 0.62\ s^{-1}$), for the gel phase

Lysozyme/wt %	Water/wt %	σ_o/Pa	$\eta(\dot{\gamma} = 0.62\ s^{-1})$/Pa s
	S/P = 21		
12.0	82.8	150	456
10.1	85.7	40	150
8.1	88.4	15	99
	S/P = 20		
11.9	83.4	210	377
10.0	86.2	58	146
9.2	87.3	20	30

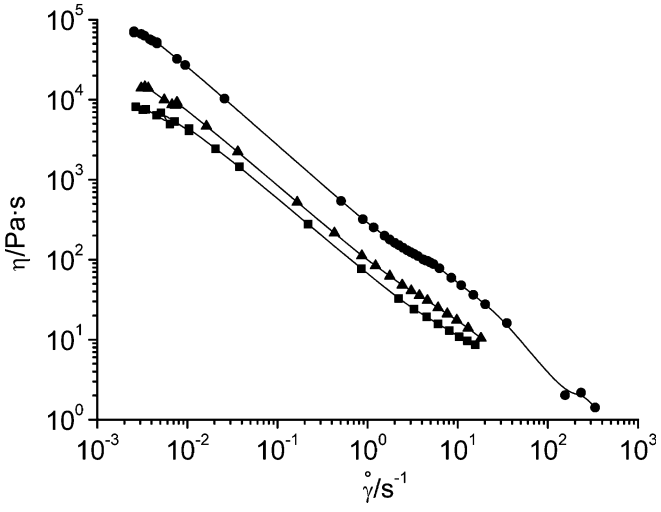

Fig. 4 Viscosity of gel samples as a function of the shear rate ($\dot{\gamma}$), for the series with S/P = 21 for different amount of water (wt %): 82.8 (*circles*); 85.7 (*triangles*); 88.4 (*squares*). The *straight lines* are guides for the eye

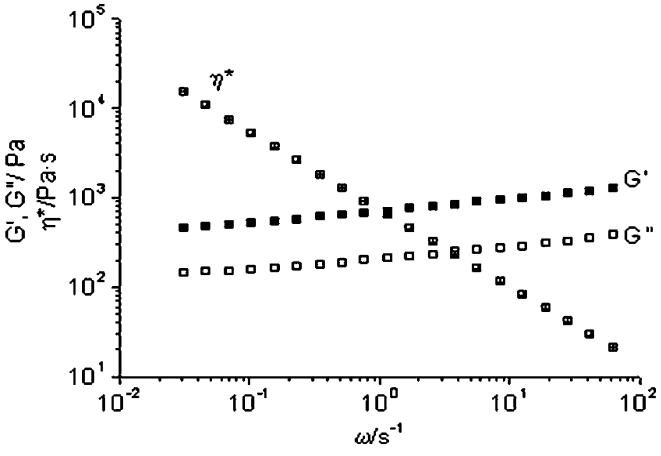

Fig. 5 Profiles of the storage modulus G', the loss modulus $G''$and the complex viscosity modulus η^* in the linear viscoelastic regime as a function of the angular frequency ω. The gel sample corresponds to the series with S/P = 20, with 87.3 wt % water

(G') and the loss (G'') moduli and of the complex viscosity modulus (η^*) from frequency sweep experiments are shown in Fig. 5.

The storage modulus is 1 decade higher in value than the loss modulus, and the complex viscosity modulus decreases in the whole range of the angular frequency with a slope of about −1. The result reflects essentially the elastic nature of this structure at any concentration in the whole range of frequencies. G' and G'' are almost parallel and depend on the oscillation frequency. Both the G' and the G'' values increase with an increase of the frequency. This observation is associated with "weak gel" behavior [16, 18, 19] and has also been described for heat-set protein gels [6, 54]. As the elastic and loss moduli do not cross each other at any frequency, the relaxation time tends to extend to infinity. This phenomenon is also associated with a yield stress value, which was determined by the flow experiments (previous section). At the time that the bluish, viscous isotropic phase was discovered in the lysozyme–SDS–water system, the authors named it the "gel phase" without having any knowledge of its rheological properties [20]. The present work characterizes the phase rheologically as a weak gel phase.

The gel structure is characterized among all sample compositions by an elastic modulus on the order of 10^2–10^3 Pa, which is the same order of magnitude as reported for the isoelectric heat-set gels of bovine serum albumin [9], β-lactoglobulin [54, 55] and the homologous lysozyme–tetramethylurea system [29] under similar protein concentrations. The frequency-dependent dynamic moduli may indicate that the gel microstructure has physical contacts that can be broken down and reformed on very long time scales [17].

In order to understand the correlation between rheological behavior and gel microstructure we carried out additional experiments by small-angle X-ray scattering. The small-angle X-ray scattering profiles do not show any measurable peaks and the intensity at low q increases enormously and a broad shoulder due to the cluster contribution is centered at 0.15 Å^{-1}. Taking into account this microsctructural picture and the structural studies carried out previously by different techniques [20, 22, 24, 25, 26, 27], one may conclude that this system forms a permanent network of protein–SDS clusters interacting reversibly through the short-range attractive interactions which may result in the weak-gel-type rheological behavior [17]. The physical contacts may also explain the phase behavior and a reversible gelling process, where the addition of SDS can redissolve the gel to an isotropic micellar solution.

Ageing

The rheological results presented in the previous sections were collected within the 3-month period after the sample preparation. These results are denoted as the initial gel stage. Knowledge of the stability of the gel with respect to time is essential for the characterization of the gel phase as well as for the possibility of its industrial application. We proposed to characterize the evolution of the gel over the time period longer than 3 months and the dynamic rheological measurements were carried out after 6 months of the sample preparation. The results indicate that all the viscoelastic parameters (G', G'' and η^*) are affected identically by

ageing. It can be inferred on the basis of the elastic modulus that the older gels always displayed higher values of all mechanical moduli than the gels at the initial stage. For example (Fig. 6), the values of the G' are larger by 1 order of magnitude compared with the G' values for the same gel at its initial gel stage. The rheological results may be understood in terms of a belated gel stage with very slow kinetics that takes place in the lysozyme–SDS–water system.

The existence of higher values of all the mechanical parameters may indicate that the belated gel material has a higher solidlike character than the initial gel material and that the solidlike character is due to a substantial enhancement of the gel strength by ageing. This behavior has also been reported for gels of the analogous lysozyme–tetramethylurea–water system [29] and the lysozyme–perfluorononanoate–water system [23]. However, in presence of SDS the gel structure needs weeks to evolve and still changes over several months. This may be due to the fact that the initial soluble protein–surfactant aggregates are charged and the repulsive interactions are of longer range than the hydrophobic attractions responsible for the aggregation and the organization in a gel network. From SANS experiments, it is clear that the gel becomes more ordered over time [28] and this effect may explain the increase of the solid character of the gel material.

In order to get additional information on the electrostatic effect on the gel network, we framed an experiment that increases the electrostatic interactions between the protein and surfactant. This was done by synthesizing a salt-free solid lysozyme–dodecyl sulfate complex that is neutral with an equimolar charge equivalent to 1 mol lysozyme to 8 mol $C_{12}SO_4^-$ [denoted as $Ly(DS)_8$] [27]. The insoluble solid complex solubilizes in water on adding excess SDS and forms both a micellar solution phase as well as a very transparent gel phase. The phase behavior of the true $Ly(DS)_8$–SDS–water ternary system is identical to that of the lysosyme–SDS–water pseudo-ternary system. The mechanical spectra of the gel recorded using the rheometer for the true ternary system are similar to the spectra obtained for the gel of the pseudo-ternary system (Fig. 5). However, gels from the $Ly(DS)_8$–SDS–water system manifest higher elasticity (i.e., higher G'/G'' ratio). We believe that the electrostatic effect changes the rheological properties. For the complex $Ly(DS)_8$, the electrostatic attraction is very strong since the lysozyme and dodecyl sulfate act as counterions to each other. On the other hand, the presence of a salt buffer in the lysozyme supplied can screen the electrostatic interactions for the pseudo-ternary system and favor a more disordered aggregation that results in a turbid gel [5], weak gel-type rheological behavior and lower elasticity.

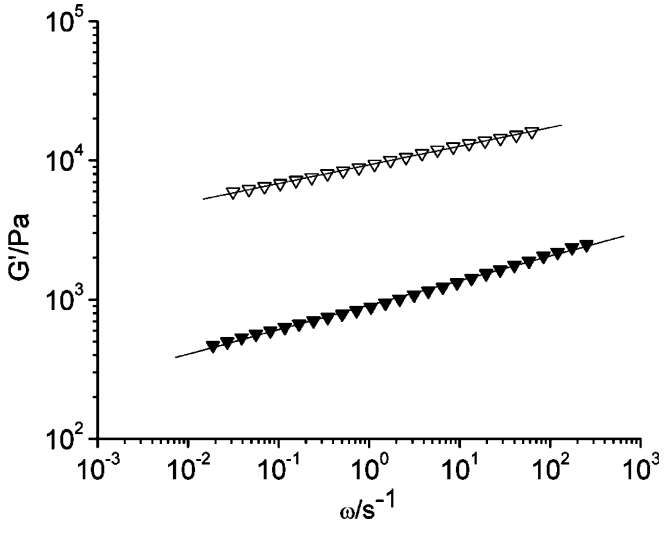

Fig. 6 Elastic modulus as a function of the angular frequency for the initial (*closed symbols*) and the later (*open symbols*) gel stages. The gel sample corresponds to the series with S/P = 20, with 83.4 wt % water

The composition effect on the viscoelastic behavior

Knowledge of the effect of the SDS and lysozyme concentrations on the different mechanical parameters can be very useful in order to correlate experimental observations with the gel structure. We only comment on the storage moduli of the initial gel structure since there is an identical composition effect on all the mechanical moduli. The G' values at $f = 0.1$ Hz ($\omega = 2\pi$f) are plotted against the surfactant-to-total molar ratio, $R = [DS^-]/([DS^-] + [Lys])$, in Fig. 7 for the series with a constant amount of protein. The gel strength is strongly dependent on both the protein content and R. Higher protein contents give higher values of all moduli (G' in the plot), which indicates that either the concentrated gels are more structured, or have a compact network. The G' value increases enormously on increasing the proportion of SDS in the sample, i.e., on decreasing the water content (Fig. 7). The stronger gel corresponds to the sample at the highest surfactant-to-total amphiphile ratio, where the G' values are over 10^4 Pa, and the yield stress value is over 60 Pa. The viscoelastic behavior of the gel phase indicates that the system may collapse or that clusters in the network may grow significantly on increasing R owing to the surfactant effect.

For the heat-set β-lactoglobulin–SDS gels, the gel strength was found to be strongly dependent on R as well. The addition of SDS leads to complex behavior, where G' passes through a maximum value on increasing R. At intermediate surfactant-to-protein ratios (i.e., where G' increases sharply as occurred in the lysozyme–

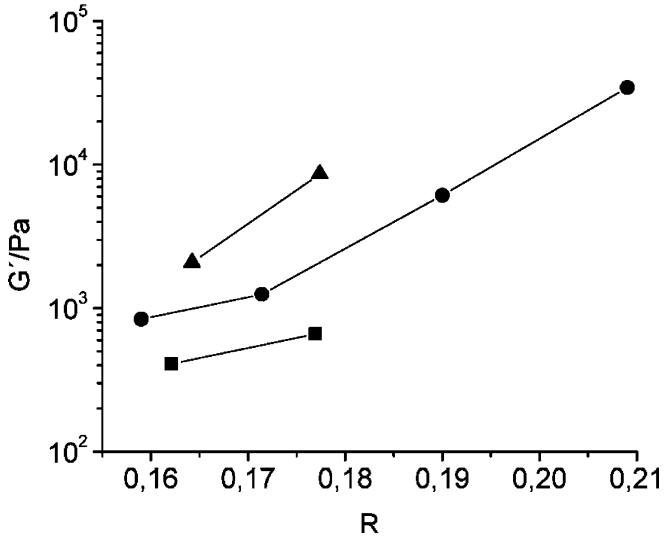

Fig. 7 Storage modulus at $f = 0.1$ Hz against surfactant-to-total amphiphile molar ratio ($R = [DS^-]/([DS^-] + [Lys])$ for the initial gel stage. Series with protein contents of 9 wt % (*squares*), 10 wt % (*circles*), and 12 wt % (*triangles*)

SDS–water system), the presence of SDS was considered as an attractive surfactant-mediated protein unfolding and additional cross-linking agent [31]. However, for the lysozyme–SDS mixtures we have not obtained any evidence of a strong unfolding process in the protein structure by Raman spectroscopy [27].

Fig. 8a,b Storage modulus (*closed symbols*) and loss modulus (*open symbols*) at $f = 0.1$ Hz as a function of temperature. **a** Series with S/P = 20: 83.47 wt % water (*circles*); 86.2 wt % water (*triangles*); 87.5 wt % water (*squares*). **b** Series with S/P = 21: 82.5 wt % water (*circles*), at $f = 1$ Hz; 85.7 wt % water (*triangles*); 88.4 wt % water (*squares*)

Effect of the temperature on the viscoelastic behavior

On heating, the gel phase composed of the surfactant–protein mixtures may undergo a phase transition or the protein may be denatured. In the absence of SDS, lysozyme in aqueous solution is denatured on heating to 78 °C at pH 6.5. We did not measure accurately the temperature at which the protein is denatured in the presence of SDS. However, we observed that the gel samples within the composition range used in this study became white at 55 °C, without applying any stress. On cooling, the samples remain permanently white [20].

We studied the effect of temperature by measuring the G' and G'' values at $f = 0.1$ Hz for samples of the series with a surfactant-to-protein ratio of 20, between 10 and 40 °C (Fig. 8a). As expected, the G' values are larger than those of the G'' values. Both moduli are almost temperature-independent and parallel to each other until a critical temperature is reached (around 32 °C). Afterwards, both the G' and the G'' values increase sharply. The critical temperature may be related to structural modifications instead of protein denaturation. We agree with the protective effect attributed to SDS with respect to thermal stability of globular proteins [31].

The samples from the series with a surfactant-to-protein ratio of 21 are more temperature-sensitive than those from the series with a surfactant-to-protein ratio of 20 since both moduli decrease gradually with increasing temperature instead of keeping constant values (Fig. 8b). This may be related to the lower elasticity of samples from the series with a surfactant-to-protein ratio of 21.The critical temperature is at least 2 °C higher than for the other series. The storage and loss moduli are not parallel in the whole temperature range. They approach each other prior to reaching the critical temperature and after that their modulus values separate again. This indicates that the gel suffers a minor struc-

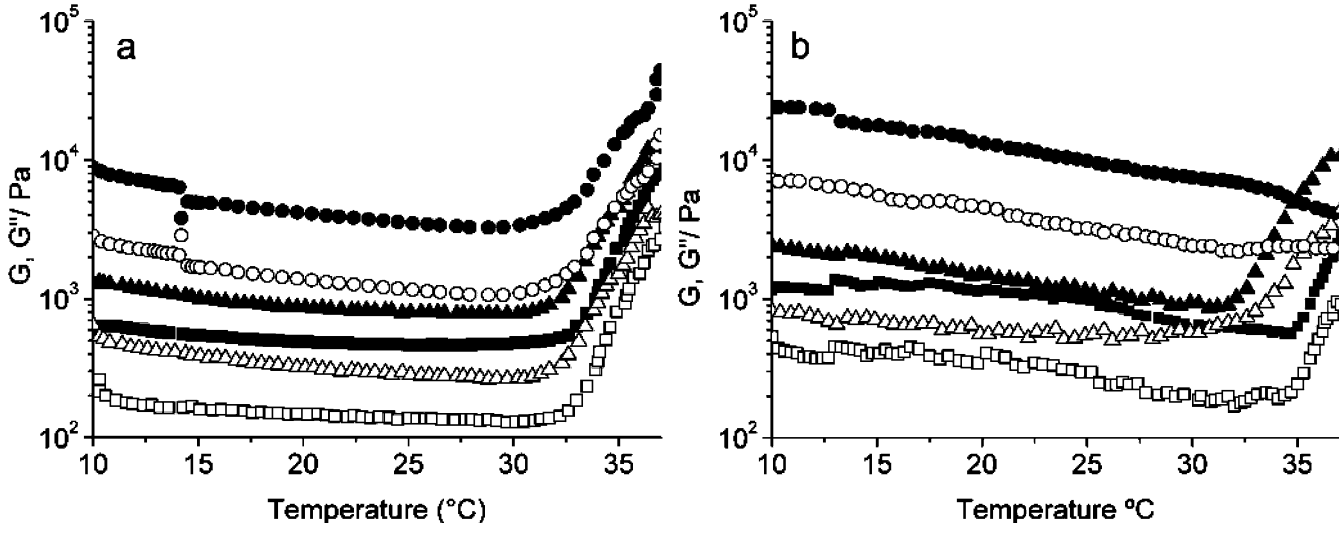

tural modification, even below the critical temperature. The modification looks to depend on the sample composition. Moreover, an inflexion in both G' and G'' is observed at about 14 °C for many samples at both surfactant-to-protein ratios, which may also be related to disruption of the structure.

Conclusions

The gel phase of the lysozyme–SDS–water system obtained by Morén et al. [20] is formed by protein–surfactant clusters organized in a network of one-dimensional growth [28]. In this paper, the gel was characterized rheologically as a weak gel. According to our rheological results the cluster units are necessarily in touch by physical contacts instead of chemical linkages. The magnitude of the G' values, the not high enough elasticity, and the turbid macroscopic appearance support this conclusion. The physical bonds may be broken and reformed on very long time scales.

We knew that the phenomenology of the gelification process is very different in the lysozyme–SDS system compared with the heat-set gels of single globular proteins. The microstructures are also different since the unfolding process has not been detected for the surfactant-induced gel. However, both types of gels manifest themselves like weak physical gels.

For the lysozyme–SDS–water system, more structured gels are obtained by increasing both the surfactant and the protein contents. A belated gel stage, which takes place after half a year, has been characterized in detail. All the mechanical parameters (G', G'' and η^* moduli) are higher compared with those of the initial gel stage; hence, ageing may lead to small structural changes in the network of the gel, which becomes less heterogeneous.

Concerning the temperature effect, the storage and the loss moduli are almost temperature-independent, and parallel to each other until a critical temperature near 32 °C is reached. The samples from the series with a surfactant-to-protein molar ratio of 21 are less elastic and more temperature-sensitive than the samples with a surfactant-to-protein ratio of 20. For the former, the gel network suffers minor structural modifications below the critical temperature.

Acknowledgements G.M. acknowledgments the Ministerio de Educación y Cultura of Spain for financial support. A. Stenstam is gratefully acknowledged for supplying the $Ly(DS)_8$ protein–surfactant complex and for valuable discussions. M. Valiente and the anonymous second reviewer are thanked for their valuable scientific comments.

References

1. Dickinson E (1993) In: Goddard ED, Ananthapadmanabhan KP (eds) Interactions of surfactant with polymers and proteins. CRC, Boca Raton, FL, p 295
2. Clark AH, Lee-Tuffnell CD (1986) In: Mitchell JR, Ledward DA (eds) Functional properties of food macromolecules. Elsevier, London, p 203
3. Clark AH, Ross-Murphy SB (1987) Adv Polym Sci 83:57
4. Clark AH, Kavanagh GM, Ross. Murphy SB (2001) Food Hydrocolloids 15:383
5. Doi E (1993) Trends Food Sci Technol 4:1
6. Arntfield SD, Bernatsky A (1993) J Agric Food Chem 41:2291
7. Kavanagh GM, Clark AH, Gosal WS, Ross-Murphy SB (2000) Macromolecules 33:7029
8. Kavanagh GM, Clark AH, Ross-Murphy SB (2002) Rheol Acta 41:276
9. Lefebvre J, Renard D, Sanchez-Gimeno AC (1998) Rheol Acta 37:345
10. Tobitani A, Ross-Murphy SB (1997) Macromolecules 30:4845
11. Tobitani A, Ross-Murphy SB (1997) Langmuir 30:4855
12. Nicolai T, Urban C, Schutenberger P (2001) J Colloid Interface Sci 240:419
13. Richardson RK, Ross-Murphy SB (1981) Brit Polym J 13:11
14. Renard D, Robert P, Faucheron S, Sanchez C (1999) Colloids Surf B Biointerfaces 12:113
15. Dickinson E (2001) Colloids Surf B Biointerfaces20:197
16. Ross-Murphy SB, Morris VJ, Morris ER (1983) Faraday Symp Chem Soc 18:115
17. Ross-Murphy SB (1995) In: Dickinson E (ed) New physico-chemical techniques for the characterization of complex food systems. Blackie, London, p 139
18. Chronakis IS, Piculell L, Borgström J (1996) Carbohydr Polym 31:215
19. Dickinson E (1997) Trends Food Sci Technol 8:334
20. Morén AK, Khan A (1995) Langmuir 11:3636
21. Morén AK, Eskilsson K, Khan A (1997) Colloids Surf B Biointerfaces 9:305
22. Morén AK, Nydén M, Söderman O, Khan A (1999) Langmuir 15:5480
23. Palacios AC, Sarnthein-Graf C, La Mesa C (2003) Colloids Surf A Physicochem Eng Asp 1
24. Morén AK, Khan A (1998) Langmuir 14:6818
25. Morén AK, Khan A (1999) J Colloid Interface Sci 218:397
26. Morén AK, Regev O, Khan A (2000) J Colloid Interface Sci 222:170
27. Stenstan A, Khan A, Wennerström H (2001) Langmuir 17:7513
28. Stenstam A, Montalvo G, Grillo I, Gradzielski M (2003) J Phys Chem B 107:12331
29. da Silva MA, Arêas EPG (2002) Biophys Chem 99:129
30. Chen J, Dickinson E, Langton M, Hermansson A-M (2000) Lebensm-Wiss Technol 33:299
31. Dickinson E, Hong S-T (1997) Colloids Surf A Physicochem Eng Asp 127:1
32. Demetriades K, McClements D (2000) Colloids Surf A Physicochem Eng Asp 161:391
33. Gekko K, Noguchi H (1979) J Phys Chem 83:2706
34. Söderman O, Jonströmer M, van Stam J (1993) J Chem Soc Faraday Trans 89:1759
35. Magid LJ, Li Z, Butler PD (2000) Langmuir 16:10028
36. Reiss-Husson F, Luzzati V (1966) J Colloid Interface Sci 21:534
37. Einstein A (1906) Ann Phys 19:289

38. Price WS, Tsuchiya F, Arata Y (1999) J Am Chem Soc 121:11503
39. Mooney MJ (1951) Colloid Sci 6:162
40. Monkos K (1997) Biochem Biophys Acta 1339:304
41. Lefebvre J (1982) Rheol Acta 21:620
42. Monkos K (2000) Biophys Chem 85:7
43. Hwang J, Kokini JL (1992) Carbohydr Polym 19:31
44. Castelain C, Doublier JL, Lefebvre J (1987) Carbohydr Polym 7:1
45. Monkos K (1994) Int J Biol Macromol 16:31
46. Valstar A, Brown W, Almgren M (1999) Langmuir 15:2366
47. Vasilescu M, Angelescu D, Almgren M, Valstar A (1999) Langmuir 15:2635
48. Gimel JC, Brown W (1996) J Chem Phys 104:8112
49. Bergström M, Pedersen JS (1999) Phys Chem Chem Phys 1:4437
50. Barnes HA, Hutton JF, Walters K (1989) An introduction to rheology. Elsevier, Oxford
51. Kinsella JE (1984) Crit Rev Food Sci Nutr 21:197
52. Greener J, Contestable BA, Bale MD (1987) Macromolecules 20:2490
53. Chen J, Dickinson E (1995) Food Hydrocolloids 9:35
54. Dickinson E (1992) An introduction to food colloids. Oxford University Press, Oxford
55. Dickinson E, Yamamoto Y (1996) J Agric Food Chem 44:1371